N-M-V DOMAINS OF CIRCULAR REINFORCED CONCRETE CROSS-SECTIONS

A.Ghersi[1], A. Recupero[2] and P.P.Rossi[3]

[1] *Professor, Dept. of Civil and Environmental Engineering, University of Catania, Italy*
[2] *Assistant Professor, Dept.* "Ingegneria Costruzioni e Tecnologie Avanzate"*, University of Messina, Italy*
[3] *Assistant Professor, Dept. of Civil and Environmental Engineering, University of Catania, Italy*
Email: aghersi@dica.unict.it, antonino.recupero@unime.it, prossi@dica.unict.it

ABSTRACT :

In the last decades a great effort has been made to obtain accurate evaluation of the resistance of reinforced concrete elements subjected to pure shear or combined internal forces including shear. In regard to this latter subject, continuum models characterized by simplified stress fields have recently been applied by some of the Authors for the evaluation of the ultimate capacity interaction diagram of rectangular reinforced concrete cross-sections undergoing combined axial force, bending moment and shear force.
The present paper constitutes the natural progress of these studies and describes an analytical tool for the calculation of the ultimate capacity interaction diagram of reinforced concrete columns with circular cross-section. The proposed method is based on the application of the static theorem of limit analysis and requires the definition of equilibrium equations and boundary conditions for geometrical and mechanical parameters. In order to validate the method, the relations developed are applied with reference to many laboratory models tested in the past and the theoretical results are compared to the experimental ones.

KEYWORDS: Shear force, axial force, bending moment, interaction diagram, circular cross-section, reinforced concrete

1. INTRODUCTION

In the attempt to provide accurate evaluation of the resistance of reinforced concrete members subjected to shear forces, researchers have often ditched the discretized models of the structural behavior which have originated from the studies of Mörsch and adopted more comprehensive continuum models. These latter models use the plastic approach and simplified stress fields to simulate the response of the materials, steel and concrete, which constitute reinforced concrete. From the first studies on this topic now (e.g. Nielsen et al., 1978) the described approach has gradually perfected and allowed the achievement of important results with moderately onerous computational tools. In particular, this method has often been used to compensate for the lack of valid code provisions relative to the assessment of the resistance of concrete members subjected to the combined action of forces including shear. In this very context, the approach has been adopted by some of the Authors to define the ultimate capacity interaction diagrams of rectangular, T and I shaped cross-sections subjected to axial force, shear force and bending moment (Recupero et al., 2003). With good accuracy in the description of the material behavior and resisting mechanisms, the study has highlighted the mutual influence of the internal forces and, in particular, explained the level of importance of the shear force for the resistance of reinforced concrete members. Furthermore, the comparison between theoretical and experimental results present in the literature proved the substantial accuracy of the method.
The present paper constitutes the natural progress of these studies and allows the definition of the ultimate capacity interaction diagram of reinforced concrete columns with circular cross-section. Under the same hypotheses as the previous studies, the Authors derive the equilibrium and boundary conditions which define the non-linear mathematical problem required for the evaluation of the interaction diagram. Then, the method is applied with reference to many laboratory models experimented in the past and their resistance is evaluated in order to assess the accuracy and reliability of the proposed procedure.

2. METHODOLOGY AND MATHEMATICAL MODEL

The proposed method allows the evaluation of the ultimate capacity of reinforced concrete columns with circular cross-section subjected to composed axial force, bending moment and shear force. The resistance of the column is evaluated through application of the static theorem of limit analysis. To this end, the behavior of concrete and steel as well is supposed to be rigid-perfectly plastic. In addition, for the sake of simplicity, the cross-section is divided into three zones (Fig. 1) in which the response of concrete and steel is described by simplified stress fields. This modeling has already been suggested by many other researchers (e.g. Nielsen et al., 1978; Hsu, 1993) and finds particular justification in well designed reinforced concrete members in which steel bars are closely spaced. Regarding the stress state of the single parts (concrete and steel bars) which constitute the reinforced concrete element, the Authors hypothesize that in the outermost zones of the cross-section (called F_1 and F_2) the longitudinal reinforcement and the concrete experience only normal stresses parallel to the longitudinal member axis and that these stresses are constant within the single zone. Instead, in the central zone (called F_3) the longitudinal and transverse reinforcements are assumed to experience stresses parallel to the axis of the steel bars. In particular, in this paper the stress field referred to the transverse reinforcement is considered inclined of an angle equal to 90° to the longitudinal member axis because the transverse reinforcement of the columns examined is always constituted by circular hoops. Finally, still in the central zone, concrete is assumed to experience principal compressive stresses which are inclined of an unknown angle θ to the longitudinal member axis.

3. ANALYTICAL FORMULATION OF THE PROBLEM

3.1 Preliminary Definitions

The dimension of the above-mentioned cross-section zones is completely defined by the angles α_1 and α_2 (**Fig.1**) which identify the upper and lower limits of the central zone F_3 of the cross-section. Furthermore, the position of the longitudinal and transverse reinforcements on the zone separation lines is established by the angles β and γ, which are linked to the angles α by means of the following relations:

$$\gamma_1 = \arcsin\left(r_l \sin\alpha_1\right); \quad \gamma_2 = \arcsin\left(r_l \sin\alpha_2\right) \tag{1}$$

$$\beta_1 = \arcsin\left(r_s \sin\alpha_1\right); \quad \beta_2 = \arcsin\left(r_s \sin\alpha_2\right) \tag{2}$$

where

$$r_l = R/(R-c); \quad r_s = R/(R-c_h) \tag{3}$$

and c_h is the cover to the circular hoops.

To obtain the stress field relative to the longitudinal reinforcement, the area A_{sl} of the longitudinal steel bars is distributed over the circumference passing through the centroids of the longitudinal steel bars. The longitudinal reinforcement λ per unit of length of this circumference is evaluated through the following relation:

$$\lambda = \frac{A_{sl}}{2\pi\left(R-c\right)} = \frac{A_{sl}}{2\pi R_l} \tag{4}$$

where R is the radius of the cross-section, R_l the radius of the circle passing through the centroids of the longitudinal steel bars and c the cover to the longitudinal reinforcement.

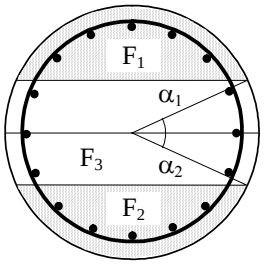

Figure 1. Definition of the zones F_1, F_2 and F_3 of the cross-section

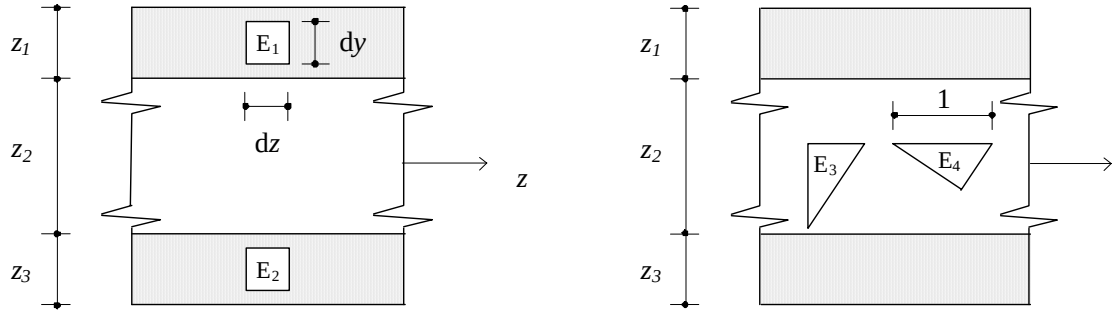

Figure 2. Identification of the elements E_1, E_2, E_3 and E_4

3.2 Equilibrium Conditions: Zones F_1 *and* F_2

To define the equilibrium conditions relative to the cross-section zones named F_1 and F_2, consider the elements E_1 and E_2 (Fig. 2) obtained by cutting the reinforced concrete member by means of two couples of planes which are spaced out to an infinitesimal quantity apart and are parallel or orthogonal to the longitudinal member axis. Owing to this, the elements E_1 and E_2 have size equal to *dy* and *dz* along the *y* and *z*-axes and depth equal to $2R\cos\alpha$ along the *x*-axis. Furthermore, they are subjected to the stresses σ_{wl} and σ_c due to longitudinal reinforcement and concrete and to the stress σ_w due to the combined action of steel and concrete (Fig. 3).
The equilibrium equation of the element E_1 along the *z*-axis may be written as ($dl = dy/\cos\gamma$)

$$\sigma_{wl1}\lambda/\cos\gamma - \sigma_{w1}R\cos\alpha - \sigma_{c1}R\cos\alpha = 0 \tag{5}$$

Starting from this equation, the normal stress σ_{w1} may be defined as

$$\sigma_{w1} = \frac{\lambda}{R\cos\alpha\sqrt{1-r_l^2\sin^2\alpha}}\sigma_{wl1} - \sigma_{c1} \tag{6}$$

As is evident from this equation, the stress σ_{w1} is constant within the zone F_1 because the stresses σ_w and σ_c are assumed constant in the same zone. Furthermore, this relation simplifies when referring to elements which are within the cover to the hoops and assumes the following form

$$\sigma_{w1}2R\cos\alpha\ dy + \sigma_{c1}2R\cos\alpha\ dy = 0 \qquad (\text{i.e. } \sigma_{w1} = -\sigma_{c1}) \tag{7}$$

Similar mathematical expressions may be obtained with reference to the element E_2 in the zone F_2. Specifically, the equilibrium along the *z*-axis may be expressed by the relation

$$\sigma_{wl2}\lambda/\cos\gamma - \sigma_{w2}R\cos\alpha - \sigma_{c2}R\cos\alpha = 0 \tag{8}$$

and thus the stress σ_{w2} as

$$\sigma_{w2} = \frac{\lambda}{R\cos\alpha\sqrt{1-r_l^2\sin^2\alpha}}\sigma_{wl2} - \sigma_{c2} \tag{9}$$

Equation (8) simplifies when referring to elements within the cover to the circular hoops

$$\sigma_{w2}2R\cos\alpha\ dy + \sigma_{c2}2R\cos\alpha\ dy = 0 \qquad (\text{i.e. } \sigma_{w2} = -\sigma_{c2}) \tag{10}$$

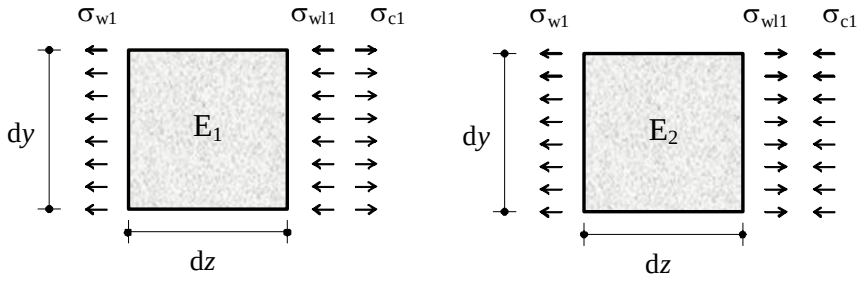

Figure 3. Stress fields in the elements E_1 and E_2

3.2 Equilibrium Conditions: Zone F_3

Consider two elements (E_3 and E_4) in the central zone (F_3) of the cross-section, as illustrated in Figure 4, and first focus the attention on the element E_3. This element is subjected to the stress σ_{wl3} due to the longitudinal reinforcement, to the stress σ_{sw} due to the circular hoops, to the tangential stress τ and to the combined normal stress σ_{w3} due to concrete and steel bars. Regarding the stress state in the entire zone F_3, the reinforcement stress is assumed to be constant; furthermore, the stress due to the circular hoops is oriented along the tangent to the hoops and thus inclined to the vertical axis of an angle β which depends on the position of the element. The angle β may be easily expressed as a function of the angle α by means of the relations

$$R\ \sin\alpha = R_l\ \sin\beta \quad \Rightarrow \quad \sin\gamma = r_s \sin\beta \quad \Rightarrow \quad \cos\beta = \sqrt{1 - r_s^2 \sin^2\alpha} \tag{11}$$

The equilibrium equations along the *y* and z-axis and the rotational equilibrium about the point O are

(transl. along the *y*-axis) $$2\frac{A_{sw}}{s}\sigma_{sw}\cos\beta\ \cos\vartheta - 2R\tau\ \cos\alpha\ \sin\vartheta = 0 \tag{12}$$

(transl. along the *z*-axis) $$\frac{2\lambda}{\cos\gamma}\sigma_{wl3}\sin\vartheta - \tau\cos\vartheta\, 2R\cos\alpha - \sigma_{w3}\sin\vartheta\, 2R\cos\alpha = 0 \tag{13}$$

(rotational equil.) $$\frac{2\lambda}{\cos\gamma}\sigma_{wl3}\frac{\sin^2\vartheta}{2} - 2\frac{A_{sw}}{s}\sigma_{sw}\cos\beta\frac{\cos^2\vartheta}{2} + \sigma_{w3}\frac{\sin^2\vartheta}{2}2R\cos\alpha = 0 \tag{14}$$

being A_{sw} the double of the cross-sectional area of the single hoop and *s* the spacing of hoops.
Substituting Equation (11) into Equation (12) gives the tangential stresses

$$\tau = \frac{A_{sw}\sigma_{sw}}{R\ s\cos\alpha}\cot\vartheta\sqrt{1 - r_s^2\sin^2\alpha} \tag{15}$$

Hence, the normal σ_{w3} may be defined by substituting Equation (15) into Equation (13)

$$\sigma_{w3} = \frac{\lambda}{R\cos\alpha\sqrt{1 - r_l^2\sin^2\alpha}}\sigma_{wl3} - \frac{A_{sw}\sigma_{sw}}{R\ s\ \cos\alpha}\cot^2\vartheta\sqrt{1 - r_s^2\sin^2\alpha} \tag{16}$$

As is evident in Equations (15-16), the normal stress σ_{w3} and the tangential stress τ cannot be constant in F_3 but are variable as a function of the angle α.
In order to evaluate the stress σ_{c3} in concrete, let us consider the element E_4. This element experiences the compressive stress σ_{c3} of concrete and the vertical component $\sigma_{sw}\cos\beta$ of the stress of the circular hoops (Fig. 4). The boundary condition $\Sigma\sigma_y = 0$ relative to the element under examination states that:

$$2\frac{A_{sw}}{s}\sigma_{sw}\cos\beta - \sigma_{c3}\sin^2\vartheta\ 2R\cos\alpha = 0 \tag{17}$$

and thus

$$\sigma_{c3} = \frac{A_{sw}\sigma_{sw}}{R\ s\ \sin^2\vartheta\ \cos\alpha}\sqrt{1 - r_s^2\sin^2\alpha} \tag{18}$$

This relation demonstrates the non-uniformity of the stress σ_{c3}. Even if not shown in figure, the non-linearity is concentrated in the parts of the zone F_3 which are far from the geometrical centre.

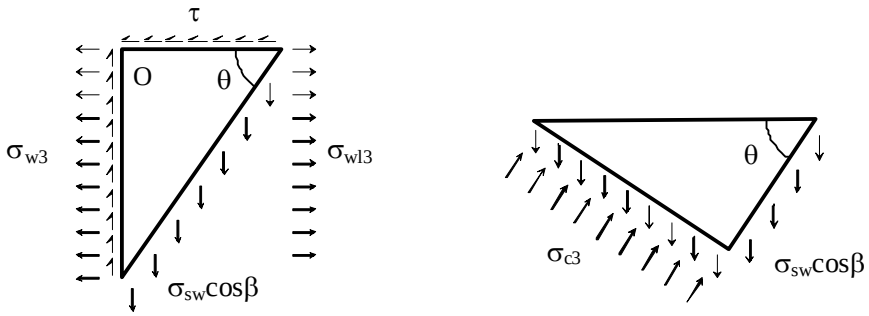

Figure 4. Stress fields in the elements E_3 and E_4

3.3. Global Equilibrium

The translational equilibrium along the longitudinal axis states that

$$N = \int_S \sigma dS = \underbrace{\int_{S_1} \sigma_{w1} dS}_{N_1} + \underbrace{\int_{S_2} \sigma_{w2} dS}_{N_2} + \underbrace{\int_{S_3} \sigma_{w3} dS}_{N_3} \tag{19}$$

being N_1, N_2 and N_3 the axial forces present in the zones F_1, F_2 and F_3.
The first contribution N_1 to the global axial force may be calculated by means of the following equation

$$N_1 = \int_{\alpha_{inf}}^{\alpha_{sup}} \sigma_{w1}(\alpha) 2R^2 \cos^2\alpha \, d\alpha = \sigma_{wl1} 2R\lambda \int_{\alpha_{inf}}^{\alpha_{sup}} \frac{\cos\alpha}{\sqrt{1-r_l^2 \sin^2\alpha}} d\alpha - \sigma_{c1} 2R^2 \int_{\alpha_1}^{\pi/2} \cos^2\alpha \, d\alpha \tag{20}$$

and the other two contributions N_2 and N_3 by the relations

$$N_2 = \sigma_{wl2} 2R\lambda \int_{\alpha_{inf}}^{\alpha_{sup}} \frac{\cos\alpha}{\sqrt{1-r_l^2 \sin^2\alpha}} d\alpha - \sigma_{c2} 2R^2 \int_{-\pi/2}^{\alpha_2} \cos^2\alpha \, d\alpha \tag{21}$$

$$N_3 = 2R\sigma_{wl3}\lambda \int_{\alpha_{inf}}^{\alpha_{sup}} \frac{\cos\alpha}{\sqrt{1-r_l^2 \sin^2\alpha}} d\alpha - \frac{2RA_{sw}\sigma_{sw}\cot^2\vartheta}{s} \int_{\varepsilon_2}^{\alpha_1} \cos\alpha \sqrt{1-r_s^2 \sin^2\alpha} \, d\alpha \tag{22}$$

The rotational equilibrium of the cross-section leads to the following equation

$$M = \underbrace{\int_{S_1} \sigma_{w1} y \, dS}_{M_1} + \underbrace{\int_{S_2} \sigma_{w2} y \, dS}_{M_2} + \underbrace{\int_{S_3} \sigma_{w3} y \, dS}_{M_3} \tag{23}$$

The contributes M_1, M_2 and M_3 to the global bending moment may be written as

$$M_1 = 2R^2 \sigma_{wl1} \lambda \int_{\alpha_{inf}}^{\alpha_{sup}} \frac{\cos\alpha \sin\alpha}{\sqrt{1-r_l^2 \sin\alpha}} d\alpha - 2R^3 \sigma_{c1} \int_{\alpha_1}^{\pi/2} \cos^2\alpha \sin\alpha \, d\alpha \tag{24}$$

$$M_2 = 2\sigma_{wl2} R^2 \lambda \int_{\alpha_{inf}}^{\alpha_{sup}} \frac{\cos\alpha \sin\alpha}{\sqrt{1-r_l^2 \sin^2\alpha}} d\alpha - 2R^3 \sigma_{c2} \int_{-\pi/2}^{\alpha_2} \cos^2\alpha \sin\alpha \, d\alpha \tag{25}$$

$$M_3 = 2R^2 \sigma_{wl3} \lambda \int_{\alpha_{inf}}^{\alpha_{sup}} \frac{\cos\alpha \sin\alpha}{\sqrt{1-r_l^2 \sin^2\alpha}} d\alpha - 2\frac{R^2 A_{sw}\sigma_{sw}}{s} \cot^2\vartheta \int_{\alpha_2}^{\alpha_1} \sin\alpha \cos\alpha \sqrt{1-r_s^2 \sin^2\alpha} \, d\alpha \tag{26}$$

Finally, the shear force may be computed by means of the following equation

$$V = \frac{R_s A_{sw} \sigma_{sw}}{s} \cot\vartheta \left[\beta_1 + \sin\beta_1 \cos\beta_1 - \beta_2 - \sin\beta_2 \cos\beta_2\right] \tag{27}$$

3.4 Mechanical and Geometrical limits

The zone separation lines must intersect the circular hoops, i.e.

$$-\alpha_{lim1} \le \alpha_1 \le \alpha_{lim1}; \quad -\alpha_{lim1} \le \alpha_2 \le \alpha_{lim1} \tag{28}$$

being $\alpha_{lim1} = \arcsin(1/r_s)$.
Furthermore, the zones F_1 and F_2 must not overlap and thus the following inequality must hold

$$\alpha_1 \ge \alpha_2 \tag{29}$$

The mechanical parameters must satisfy the following relations

$$0 \le \sigma_{c1} \le f_{cd1}; \quad 0 \le \sigma_{c2} \le f_{cd1}; \quad 0 \le \sigma_{c3max} \le f_{cd2} \tag{30}$$

$$\sigma_{wl1} \le f_{yd}; \quad \sigma_{wl2} \le f_{yd}; \quad \sigma_{wl3} \le f_{yd}; \quad \sigma_{sw} \le f_{yd} \tag{31}$$

where f_{ck} is the characteristic value of the compressive strength of concrete, f_{yk} the characteristic value of the yield strength of steel and

$$f_{cd1} = 0.85\frac{f_{ck}}{\gamma_c}; \quad f_{cd2} = 0.6\left(1 - \frac{f_{ck}}{250}\right)\frac{f_{ck}}{\gamma_c} \qquad (\gamma_c=1.6) \qquad (32)$$

Finally, in accordance with the Italian application document to Eurocode 2, the angle of the compressive stress on the concrete of the central zone F_3 is assumed as variable between the following limits:

$$1 \le \cot\vartheta \le 2 \qquad (33)$$

4 INTERACTION DOMAINS

The resistance of reinforced concrete elements is evaluated by means of ultimate capacity interaction diagrams. The coordinates of the generic point of this diagram are calculated by mathematical non-linear programming problems which include the aforementioned equilibrium and boundary equations. With the aim of obtaining the interaction diagram, the maximum values of two of the internal actions under examination (e.g. axial force and bending moment) are first separately calculated. Hence, the range of values of these two variables is discretized and the maximum and minimum possible values of the shear force are calculated for each couple of the variables selected. The mathematical problem is non linear and, therefore, the solution of the problem depends on the starting values of all the parameters of the problem. In order to find a safe value of the shear resistance, the mathematical problem is solved with reference to many starting values of the parameters and the lowest value of the shear force is assumed as the shear capacity of the member.

4.1. Example

The proposed method is first applied to a circular reinforced concrete column characterized by R= 30 cm, A_{sl}=30.54 cm^2 (12 bars with diameter equal to 18 mm), c=5 cm, A_{sw}=0.50 cm^2 (hoops with diameter equal to 8 mm) and s=10 cm. In addition, the compressive strength of the concrete is characterized by f_{cd1} =11.02 MPa and the yield strength of the longitudinal and transverse reinforcements by f_y=374 MPa.
The ultimate capacity interaction diagram of the cross-section is reported in Figure 5 with reference to an axial force of 700 kN. To define synthetically the ultimate capacity interaction between bending moment and shear force, the domain is divided into four zones which are labeled with numbers from 1 to 4. The segments which separate the zones identify points of the interaction diagram which are characterized by reductions of the ultimate bending moment equal to 25%, 50% and 75%. With reference to the points A and B of Figure 5, Figure 6 shows the stress state of concrete and steel bars and the dimensions of the zones F_1 to F_3 of the cross-section. To highlight the influence of the longitudinal reinforcement on the resistance of the cross-section, the interaction diagram is reported in Figure 7 with reference to reinforcement ratios equal to 0.20, 0.30 and 0.40 cm²/m. The influence of the transverse reinforcement is also apparent in Figure 7 where the interaction diagrams are plotted for hoop spacing equal to 5 and 10 cm. Even if not shown in the figure, the dimension of the domain reduces for very high values of the axial force.

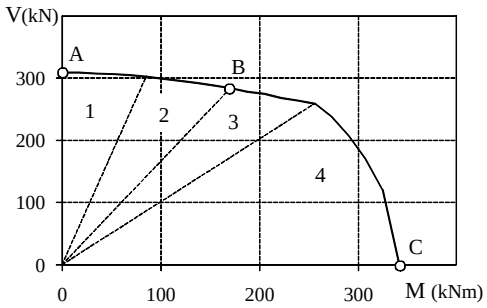

Figure 5. Evaluation of the control parameter as a function of the aspect ratio *L/D*

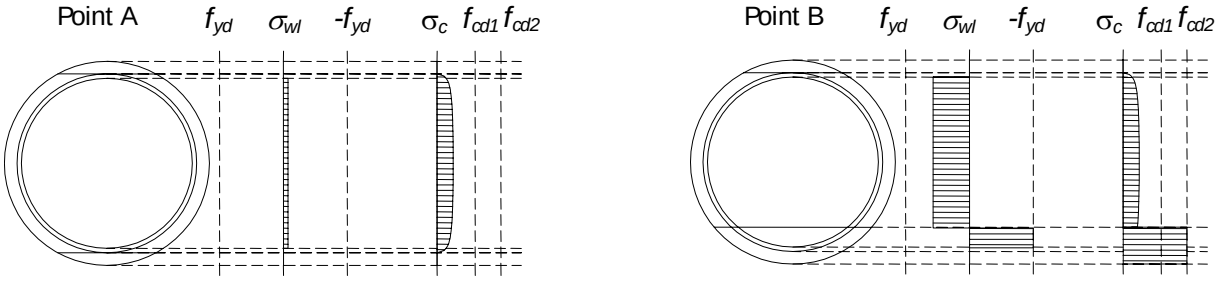

Figure 6. Stress relative to points A and B of the interaction diagram

5. COMPARISON WITH LABORATORY TESTS

The results of many laboratory tests have been compared here with those of the proposed analytical method. The laboratory tests refer to different amounts of longitudinal and transverse reinforcements and are described in detail in Ghee et al. (1989), Ascheim and Moehle (1992), Priestley and Benzoni (1996), Calderone et al. (2000), Chai et al. (1991), Berry et al. (2004), Kowalsky et al,. (1999), Kunnath et al. (1997), Lim and McLean (1991), Lehman and Moehle (1998), Priestley et al. (1994a), Priestley et al. (1994b) and Wong et al. (1993). The cross-section geometrical properties and the mechanical characteristics of concrete and steel considered in the application of the proposed method are deduced from these papers.

A dedicated index has been defined for comparison of theoretical and experimental results. Specifically, on the *M-V* interaction diagram relative to the axial force of the experimental test the Authors have marked the point corresponding to the maximum experimental values of bending moment and shear force (M_{exp}, V_{exp}). Hence, a segment has been drawn from the origin of the coordinate system to the point marked. Owing to the static determinacy of the scheme, the points of these segments represent the internal actions experienced by the column during the test. The intersection of this segment with the *M-V* diagram defines the couple of internal actions corresponding to the prediction of the ultimate capacity of the member. If O indicates the origin of the coordinate system, P_1 the point of coordinates (M_{exp}, V_{exp}) and P_2 the point of coordinates (M_{calc}, V_{calc}) the parameter adopted for comparison is

$$\delta = \frac{\overline{OP_1}}{\overline{OP_2}} \tag{34}$$

The values assumed by this parameter are reported in Figure 8. In the same figure the values are differentiated depending on the zone of the domain in which the points of coordinates (*M*, *V*) fall.

With few exceptions the analysis highlights a good accord between theoretical and experimental results. This is evident in Figure 8 where the parameter is plotted as a function of the aspect ratio L/D, i.e. of the ratio of the shear span to the column diameter. The accord is obviously less accurate in elements with low aspect ratio. However, it should be noted that in these cases the prediction is always on the safe side. This is not surprising because the resisting mechanism of these latter models is chiefly characterized by direct travel of the force to the support, i.e. by arch action, while that simulated by the proposed model refers to the so called beam action.

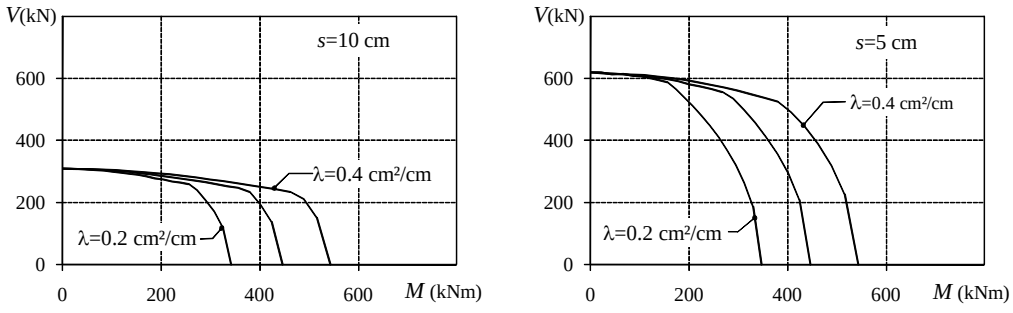

Figure 7. *M-V* domains for different longitudinal and transverse ratios (*N*=700 kN)

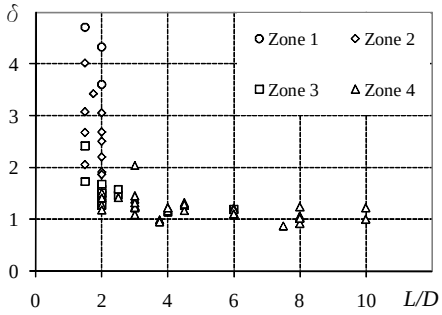

Figure 8. Evaluation of the control parameter as a function of the aspect ratio *L/D*

CONCLUSIONS

The paper proposes a mathematical model for the evaluation of the resistance of columns with circular cross-section subjected to combined axial force, shear force and bending moment. The model is based on the plastic approach and on the schematization of the resisting mechanisms by means of stress fields. In order to evaluate the reliability of the method the resistance of many columns tested in the last decades has been predicted by the theoretical approach. The comparison highlights that the theoretical model generally provides good estimates of the experimental results as long as the arch effect does not govern the structural behavior.

REFERENCES

Ascheim and Moehle 1992. *Shear Strength and Deformability of RC Bridge Columns Subjected to Inelastic Cyclic Displacement. Report n° UCB/EERC 92/04*, Earth. Eng. Research Center, University of California at Berkeley, USA.

Berry, M., Parrish, M., Eberhard, M. 2004. *PEER Structural Performance Database.* Pacific Earth. Eng. Research Center.

Calderone, A.J., Lehman, D.E., Moehle, J.P. 2000. *Behavior of Reinforced Concrete Bridge Columns Having Aspect Ratios and Varying Lengths of Confinement.* PEER Report 2000/08, pp. 136.

Chai, Y.H., Priestley, M.J.N., Seible, F. 1991. *Seismic Retrofit of Circular Bridge Columns for Enhanced Flexural Performance.* ACI Structural Journal, vol. 88, n° 5, pp. 572-584

Ghee, A. B., Priestley, M.J.N., Paulay, T. 1989. *Seismic shear strength of circular reinforced concrete columns.* ACI Structural Journal, vol. 86, pp. 45 – 59.

Priestley, M.J.N., Benzoni, G. 1996. *Seismic Performance of Circular Columns with Low Longitudinal Reinforcement Ratios.* ACI Structural Journal, vol. 93, n° 4, pp. 474 – 485.

Hsu, T.T.C. 1993. *Unified Theory of Reinforced Concrete.* CRC

Kowalsky, M.J., Priestley, M.J.N., Seible, F.. 1999. *Shear and Flexural Behavior of Lightweight Concrete Bridge Columns in Seismic Regions.* ACI Structural Journal, vol. 96, n° 1, pp. 136 – 148.

Kunnath S.K., El-Bahy, A., Taylor, A.W., Stone, W.C. 1997. *Cumulative Seismic Damage of Reinforced Concrete Bridge Piers. Technical Report NCEER-97-0006*, National Center for Earthquake Research, pp.147.

Lehman, D.E., Moehle, J.P. 1998. *Seismic Performance of Well-Confined Concrete Bridge Columns.* Pacific Earthquake Engineering Research Center, PEER Report 1998/01, pp. 205.

Lim, K.Y, McLean, D.I. 1991. *Scale Model Studies of Moment-Reducing Hinge Details in Bridge Columns.* ACI Structural Journal, vol. 88, n° 4, pp. 465– 474.

Nielsen, M.P., Braestrup, M.W., Bach, F. 1978. Rational analysis of shear in reinforced concrete beams. IABSE Proceedings.

Priestley, M.J.N., Seible, F., Xiao, Y., Verma, R. 1994a. *Steel jacket retrofitting of reinforced concrete bridge columns for enhanced shear strength- Part1: Theoretical consideration and test design.* ACI Structural Journal, vol. 91, pp. 394 – 405.

Priestley, M.J.N., Seible, F., Xiao, Y., Verma, R. 1994b. *Steel jacket retrofitting of reinforced concrete bridge columns for enhanced shear strength- Part2: Test results and comparison with theory.* ACI Structural Journal, vol. 91, pp. 537 – 550.

Recupero, A., D'Aveni, A., Ghersi, A. 2003. *N-M-V Interaction Domains for Box I-shaped Reinforced Concrete Members*, ACI Structural Journal, vol. 100, n° 1, pp. 113-119.

Recupero A., D'Aveni, A., Ghersi, A. 2005. *N-M-V Interaction Domains for Prestressed Concrete Beams*, Journal of Structural Engineering, vol. 131, n° 9.

Wong, Y., Paulay, T., Priestley, M.J.N. 1993. *Response of Circular Reinforced Concrete Columns to Multi-Directional Seismic Attack.* ACI Structural Journal, vol. 90, n° 2, pp. 180 – 191.